Biointerface Research in Applied Chemistry
Open-Access Journal (ISSN: 2069-5837)

Article
Volume 13, Issue 5, 2023, 428
https://doi.org/10.33263/BRIAC135.428

Use of Low-Cost Materials as Adsorbent for Fluoride (F^-) Mitigation

Moumita Rani Ghosh [1], Sneha Prabha Mishra [1,*]

1 Department of Chemistry, Siksha 'O' Anusandhan (Deemed to be University), Bhubaneswar, 751 030, India
* Correspondence: spm_iter@rediffmail.com (S.P.M.); mistimitra@yahoo.co.in (M.R.G.)

Scopus Author ID57211529060

Received: 23.07.2022; Accepted: 10.09.2022; Published: 15.12.2022

Abstract: Adsorption technology has been considered to be an effective technology for the removal of F^- from the aqueous solution. In adsorption technology, varieties of materials can be taken as adsorbents. But, using natural, low-cost materials is being prioritized more. The efficiency of these natural, low-cost materials can be increased further by modifying their surfaces. So, in the present investigation, F^- has been removed from the synthetic aqueous solution using four modified/unmodified low-cost adsorbents. These are heat-treated bauxite (HTB), hydrochloric acid-treated water filter carbon waste (HFCW), hydrochloric acid-treated *Lagenaria siceraria* peel (HLSP), and sand without any modifications. F^- adsorption was carried out on all these adsorbents separately at identical conditions. The effect of different adsorption parameters on all the adsorption studies was evaluated. The data were fitted to different isotherm/kinetic equations. HTB was found to be the best out of all, and further studies were carried out using HTB. The Langmuir adsorption capacity for HTB was found to be 3.1 mg/g. F^- loaded HTB could be regenerated using NaOH and could be reused for up to 3 cycles. The studied adsorbents can be used to treat real F^- polluted water.

Keywords: adsorption; fluoride; low-cost adsorbent; Langmuir isotherm; regeneration; reuse.

1. Introduction

Fluorine is the 13th most abundant element in the earth's crust, and its level in the earth's crust is 0.3 g/kg. It also exists as F^- in different minerals, out of which fluorspar, fluorapatite, and cryolite are the most common. The major source of F^- in different water sources is due to the dissolution of these F^- containing geo-chemical rocks [1]. Therefore, F^- is present in almost all water sources, including groundwater ranging from negligible amounts to more than 10 mg/L. F^- also enter into the aqueous system through various anthropogenic causes like oil refining, coal burning, brick-making industries, steel factories, and phosphate fertilizer plants [2]. F^- is an essential constituent for human beings and animals as it helps in the mineralization of teeth and bones and prevents dental caries/cavities. The effect of F^- is considered to be protective when its concentration in the aqueous solution is up to 1 mg/L [3].

But, when F^- concentration in the aqueous solution is high, it causes critical health hazards like skeletal and dental fluorosis. More than 260 million people are fluorosis affected worldwide [4]. Therefore, removal of F^- from aqueous solution is required when its concentration exceeds the maximum contamination level in the aqueous medium prescribed by World Health Organization (W.H.O.), i.e., 1.5 mg/L [5]. For the treatment of highly concentrated F^- different advanced treatment processes such as reverse osmosis, membrane-

based methods, coagulation/precipitation, and ion exchange are applied. Most of these available defluoridation techniques are costly, complex, and technically difficult to be accepted in rural areas [6]. Therefore, it is necessary to go for a cheap, easy, and safe method.

Adsorption is one such method that is cheap, highly efficient, easily accessible, eco-friendly, and does not need costly equipment and skilled manpower. One of the added advantages of the adsorption process is the vast choice of different low-cost materials as adsorbents increasing the cost-effectiveness of the process [7]. Sometimes, the uptake or removal capacities of low-cost materials are very less. In that case, modification of the adsorbent materials makes the system more efficient [8]. Therefore, in the present investigation F^- has been removed from the synthetic aqueous solution using various low-cost materials after their modifications. Different low-cost materials, either modified or unmodified, have also been tried by different researchers for the defluoridation of aqueous solutions [9,10].

Considering the above, the present research aims (a) to choose four low-cost materials from four different sources (b) to modify their surfaces simply by acid/heat treatments for improvement of their uptake capacities so that their cost will not be affected much (c) to choose the better one for each adsorbent concerning their uptake capacities out of modified or unmodified forms (d) to characterize the selected adsorbents (e) to find out the optimum condition for F^- adsorption on the selected adsorbents (f) to study different adsorption isotherm/kinetic for the said adsorption processes (g) selection of the best adsorbent out of four and to utilize the same for reuse, regeneration.

2. Materials and Methods

2.1. Adsorbate and adsorbents.

Analytical grade NaF was used to prepare 1 g/L F^- stock solution. Four low-cost adsorbents were selected from four different sources. These are domestic water filter carbon waste, *Lagenaria siceraria* (bottle gourd) peel, bauxite, and sand. All the adsorbents were washed thoroughly after collection and air-dried, followed by oven dried for excess moisture removal. The adsorbents were modified simply by heat and acid treatments without increasing the cost much. For heat treatment, samples were kept at different temperatures (200 – 700^{o}C) in a muffle furnace, and for acid treatment, the adsorbents were treated by 0.1M HCl/0.1M H_2SO_4 for 1 d at the solid:liquid ratio of 2:5 g/mL. The adsorbents were properly stored in air-tight sample bottles for subsequent use.

2.2. Methods of characterization of the adsorbents.

The Fourier Transform Infrared (FTIR) spectra of the four selected adsorbents were carried out using JASCO FTIR instrument – 4100. The point of zero charge (pzc) of the said adsorbents was determined using the solid addition method. The specific surface areas of the adsorbents were determined by Brunauer–Emmett-Teller (BET) method using Micromeritics ASAP 2020 BET analyzer at 77K. The % moisture content and mass loss due to ignition were found by keeping the samples at 105^{o}C and 600^{o}C, respectively, for 2 h. The pH of the adsorbents was determined by stabilizing the adsorbents in distilled water for 1 h at solid:liquid ratio of 10 g/L. The displacement method was used for density measurement [11].

2.3. Batch adsorption studies.

The pH of the solution was adjusted either with 0.1M HCl or 0.1M NaOH. The solutions along with the required amount of adsorbents were agitated using a magnetic stirrer (temperature controlled). After adsorption studies, from time to time, samples were collected, filtered by Whatman (no 1) filter paper, and analyzed for F^-. Most of the studies were carried out at stirring speed – 200 rpm, pH - 5, F^- concentration - 10 mg/L, room temperature, and adsorbent concentration – 5 g/L. For the confirmation of results, the experiments were conducted in triplicates, and the averages were used for calculations.

2.4. Desorption studies.

F^- loaded adsorbent (2.84 mg/g) was prepared after repeated contact of 20 mg/L F^- solution with the adsorbent at a solid:liquid ratio of 10 g/L in batch mode at optimum condition. Different desorbing agents (0.1M), like HCl, H_2SO_4, HNO_3, NaOH, and Na_2CO_3, were used in regeneration experiments. The desorption experiments were carried out at solid:liquid ratio of 5 g/L at room temperature.

2.5. Analysis.

F^- analyses from the aqueous solution were carried out by SPADNS method with the help of SL-244 (ELICO) double-beam UV-Visible Spectrophotometer. The molar absorption coefficients of the colorless F^--SPADNS complexes were determined at 570 nm wavelength [12].

3. Theory/Calculation

3.1. Calculation of % moisture content, % mass loss on ignition, % adsorption and mg/g F^- uptakes.

$$\% \text{ moisture content / \% mass loss on ignition} = \frac{W_2 - W_3}{W_2 - W_1} x100 \quad (1)$$

$$\text{Adsorption (\%)} = [(C_o - C_e)/C_o] \times 100 \quad (2)$$

$$F^- \text{ uptake (mg/g)} = [(C_o - C_e)V]/M \quad (3)$$

where W_1 - Mass of the empty crucible, g
W_2 - Mass of the sample with crucible prior to heating, g
W_3 - Mass of the sample with crucible after heating, g.
C_o - Initial F^- concentration in the solution, mg/L
C_e - F^- concentration at equilibrium, mg/L
V - Volume of the solution, L and
M - Mass of the adsorbent, g.

3.2. Calculation of standard deviation and data accuracy.

Standard deviation was calculated using the following formula, as shown in equation 4 [13].

$$s = \sqrt{\frac{\Sigma (X - \bar{x})^2}{n - 1}} \quad (4)$$

where S - Standard deviation

X - Each value

$\bar{x}$ - Mean value

n - No. of values

A low standard deviation indicates the closeness of the values with their mean values. For a good fit, the standard deviation should be < 1.

3.3. Determination of different thermodynamic, kinetic, and isotherm parameters.

Determining thermodynamic, kinetic and isotherm parameters is essential as these are the key points to know about the adsorbents' physicochemical properties and the adsorption processes' mechanism [14]. Therefore, the description of the equations used to determine all such parameters is highlighted in Table 1.

Table 1. Description of the thermodynamic, kinetic, and isotherm parameters.

Sl no.	Name of the models	Linear equations	Graph plotted	Conclusions	Significance	Eqn. No.
1	Arrhenius equation	$\ln k = \ln A - {}^{Ea}/_{RT}$	X axis: 1/T Y axis: lnk	Slope gives E_a Intercept gives A	Determination of activation energy	(5)
2	van't Hoff equation	$\ln K_D = {}^{\Delta S}/_{R} - {}^{\Delta H}/_{RT}$	X axis: 1/T Y axis: $\ln K_D$	Slope gives ΔH Intercept gives ΔS	Determination of enthalpy and entropy changes	(6)
3	Gibbs Free energy equation	$\Delta G = \Delta H - T\Delta S$	--	--	Determination of Gibbs free energy change	(7)
4	Langmuir adsorption isotherm (linear)	${}^{C_e}/_{q_e} = {}^{1}/_{q_m b} + {}^{C_e}/_{q_m}$	X axis: C_e Y axis: ${}^{C_e}/_{q_e}$	Slope gives q_m Intercept gives b	Determination of maximum monolayer adsorption capacity	(8)
5	Freundlich equation (linear)	$\log q_e = \log K + {}^{1}/_{n} \log C_e$	X axis: $\log C_e$ Y axis: $\log q_e$	Slope gives n Intercept gives K	Determination of Freundlich constants	(9)
6	Lagergren's pseudo first order equation	$\log(q_e - q_t) = \log(q_e) - \left({}^{k_1}/_{2.303}\right) t$	X axis: t Y axis: $\log(q_e - q_t)$	Slope gives k_1 Intercept gives q_e	Determination of pseudo 1st order rate constant	(10)
7	Ho & McKay pseudo second order equation	${}^{t}/_{q_t} = {}^{1}/_{k_2 q_e{}^2} + {}^{1}/_{q_e} t$	X axis: t Y axis: ${}^{t}/_{q_t}$	Slope gives q_e Intercept gives k_2	Determination of pseudo 2nd order rate constant	(11)
8	Morris-Weber equation	$q_t = R_{id} t^{1/2} + C$	X axis: $t^{1/2}$ Y axis: q_t	Slope gives R_{id} Intercept gives C	Determination of intra particle transport rate constant	(12)
9	Dubinin-Radushkevich (D.R.) isotherm	$\ln q_e = \ln X'_m - K' \epsilon^2$	X axis: ϵ^2 Y axis: $\ln q_e$	Slope gives K' Intercept gives X'_m	Determination of adsorption energies	(13)
10	Temkin isotherm	$q_e = B \ln A_T + B \ln C_e$	X axis: $\ln C_e$ Y axis: q_e	Slope gives B Intercept gives A_T	Determination of heat of sorption	(14)

where k - Rate constant of the reaction, g/mg/min;

A – Arrhenius frequency factor

E - Energy of activation, kJ/mol

T – Absolute temperature, K

R - Universal gas constant, J/K/mol

K_D - Distribution coefficient = $\frac{Adsorbateconcentrationonadsorbent\left(\frac{mg}{g}\right)atequilibrium}{Adsorbateconcentrationinsolution\left(\frac{mg}{L}\right)atequilibrium}$

ΔS - Entropy change, kJ/K.mol

ΔH - Enthalpy change, kJ/mol

ΔG – Gibbs free energy change, kJ/mol

b (constant) - Adsorption energy, L/mg

q_m - Adsorption capacity, mg/g

C_e – Equilibrium F^- concentration, mg/L

q_e – F^- adsorbed at equilibrium per unit weight of adsorbent, mg/g

K - Adsorption capacity, mg/g,

n - Adsorption intensity (constant)

q_t – F^- adsorbed at time t, mg/g

k_1 - Rate constant (pseudo 1st order), 1/min.

k_2 - Rate constant (pseudo 2nd order), g/mg/min

R_{id} - Intra particle diffusion rate constant of adsorption, $mg/g/min^{0.5}$

C – Boundary layer thickness, mg/g

Є - Polanyi potential = RT ln $(1+1/C_e)$

$X_m^{\cdot}$ - D.R. isotherm uptake capacity of adsorbent, mg/g

K' –Adsorption energy related constant, mol^2/kJ^2

B - Heat of adsorption related constant, J/mol

A_T - Temkin equilibrium binding constant, L/g

$$R_L = {}^{1}/_{(1+bC_o)} \quad (15)$$

where R_L- Separation parameter

C_o - Initial F^- concentration in the solution, mg/L

b - Langmuir isotherm parameter

According to McKay et al., for favorable adsorption processes, R_L values should lie between 0 and 1.

4. Results and Discussion

4.1.Modification of low-cost adsorbents.

Heat treatment did not affect domestic water filter carbon waste (FCW) and *Lagenaria siceraria* peel (LSP). 0.1M HCl treated FCW gave better F^- adsorption (22.74 %) compared to 0.1M H_2SO_4 treated FCW (9.64%). Treatment of LSP with 0.1M HCl was better (57.8%) compared to 0.1M H_2SO_4 (42.44%). The genus *Lagenaria* is mainly composed of cellulose and lignin. Cellulose is rich in hydroxyl groups, and lignin is mainly alcohol. During acid modification, the H^+ ions of acids may react with these hydroxyl groups and produce –OH2+ as per the reaction in equation 16 [15].

$$-OH + H^+ \rightarrow -OH_2^+ \quad (16)$$

So the adsorption of negatively charged F^- ion is facilitated due to the electrostatic force of attraction. Heat treatment to bauxite gave better results compared to either of the acid treatments. Modification at 400°C gave the best result for F^- adsorption (95%), whereas F^- uptake by unmodified bauxite was only 16.5 %. The increased F^- adsorption on bauxite after heat treatment may be due to dehydration and removal of volatile substances present on the bauxite surface so that its surface area and porosity increase. At temperatures higher than 400°C, the % of adsorption decreases may be due to the formation of compact mineral phase corundum (Al_2O_3) [16]. Sand is a granular material that occurs naturally and is composed of

minerals and finely divided rock particles. Heat/acid treatments did not work on sand. So, it is considered harder and chemically inert [17].

So, finally, 0.1M HCl treated water filter carbon waste (HFCW), 0.1M HCl treated *Lagenaria siceraria* peel (HLSP), heat-treated bauxite (HTB), and sand without any modifications were taken for further studies. The F^- uptakes on different adsorbents before and after modifications are shown in Figure 1. From the figure, it is obvious that HTB is the best adsorbent for F^- removal.

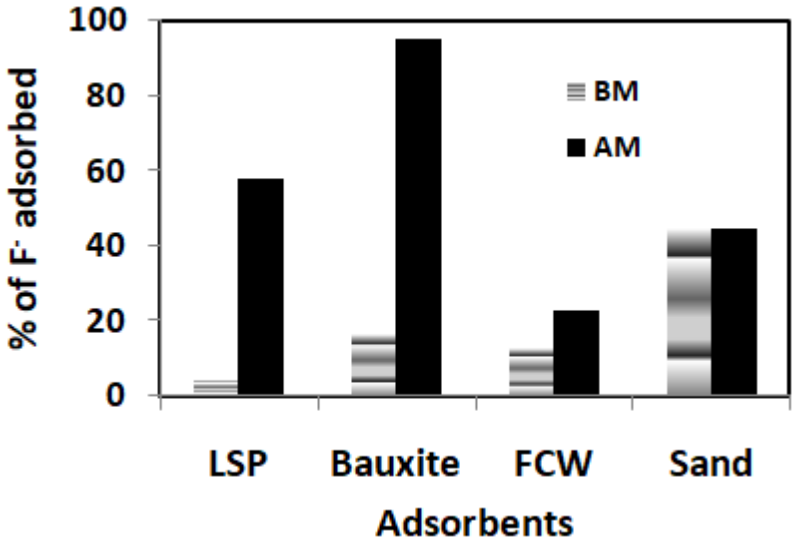

Figure 1. Effect of modifications of the selected adsorbents on % of F^- adsorptions (BM – Before modification and AM – After modification).

4.2. Characterization of the adsorbents under study.

4.1.1. Fourier Transform Infrared (FTIR) Spectroscopy.

The FTIR spectra of all the selected adsorbents are shown in Figure 2.

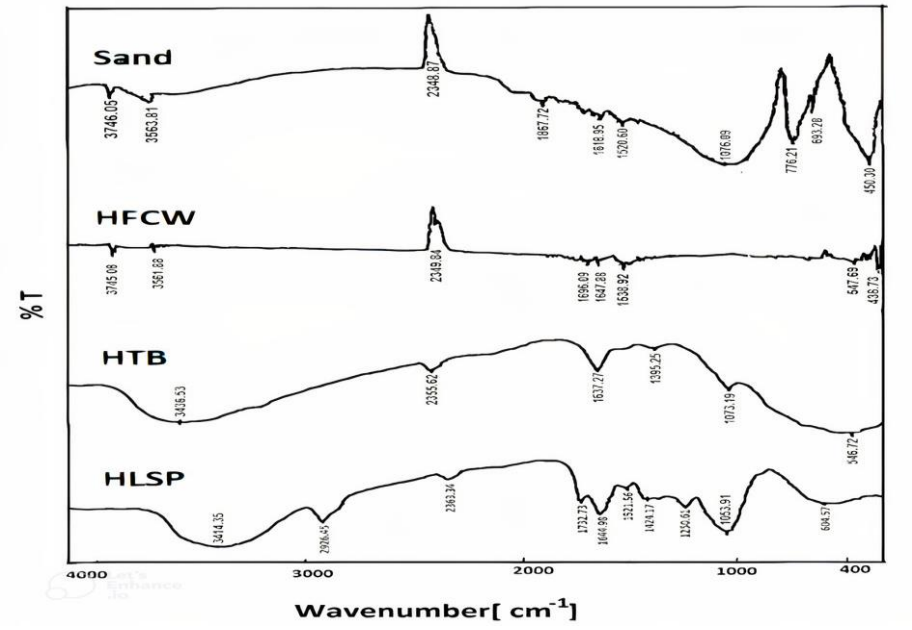

Figure 2. FTIR spectra of the four adsorbents under study.

FTIR spectra of HLSP and HTB are quite similar, whereas that of HFCW and sand are similar. In the case of HFCW and sand, no strong and broad peaks are observed at around 3400

cm^{-1} wave no., which indicates the absence of the –OH group. Only medium peaks are observed at 2347.91 cm^{-1} and 2348.87 cm^{-1} wave no. for HFCW and sand respectively. But in the case of HLSP and HTB, strong and wide peaks are observed at 3414.35 and 3436.53 cm^{-1}, respectively. It indicates OH stretch bond and H bonded structures like alcohols and phenols. In HTB it may be due to –OH group of Gibbsite, the main mineral of bauxite. So, from the above observation, it is clear that OH functional groups are present in both HLSP and HTB whereas it is absent in the other two [18]. It has also been observed that the F^- removal capacity of HLSP and HTB is more compared to HFCW and sand. So F^- removal from the aqueous solution may be mainly due to the surface complexation method. F^- exists as fluoride (F^-) or bifluoride (HF_2^-) in natural water, depending on the pH of the solution [19]. The surface complexes formed in between -OH groups of the adsorbents and F^- can be interpreted as equations 17 and 18.

$$S - OH + H^+ + F^- \leftrightarrow [S - OH_2^+ - F^-] \quad (17)$$

$$S - OH + H^+ + HF_2^- \leftrightarrow [S - OH_2^+ - HF_2^-] \quad (18)$$

where S-OH is the adsorbent surface with –OH group and [S - OH_2^+ - F^-] and [S - OH_2^+ - HF_2^-] are the surface complexes [20]. F^- adsorption may also occur due to the substitution of –OH group on the adsorbent surface by F^- ions.

4.1.2. Other physicochemical parameters.

The physicochemical properties such as pH, % loss of mass on ignition, % moisture content, density, and surface area for the studied adsorbents are shown in Table 2 and are comparable to the other reported data [21]. The pzc of HTB is a maximum (7.8) out of all. That means the surface of HTB remains positive up to a wide pH range compared to other adsorbents. This may be one important reason for the maximum adsorption of negatively charged F^- ion on HTB surface. The B.E.T. surface area of HTB is also the highest, as shown in Table 2.

Table 2. Different physicochemical parameters.

Properties	HLSP	HTB	HFCW	Sand
pzc	3.4	7.8	5.6	3.1
pH	6.3	6.0	7.02	7.95
% Moisture content	2.22	3.3	5.0	3.4
% Loss of mass due to ignition	90	10.6	68.4	70.0
Surface area (m^2/g)	44.6	71	39	32.6
Density (g/cm^3)	0.386	1.66	1.25	1.46

4.2. Effect of different adsorption parameters.

4.2.1. Effect of contact time.

The effect of contact time was studied within the range of 0 to 250 minutes keeping other parameters constant. The % of F^- adsorption increases up to their optimum contact times and thereafter remains constant, as shown in Figure 3. It is because, initially, all the functional groups present on the adsorbent surfaces remain free. With the passage of time, when adsorbent surfaces get saturated, no more adsorptions take place [22]. The contact time at which the adsorption surface becomes saturated is known as the optimum contact time. The optimum contact times for F^- adsorption on HFCW and sand are 60 minutes, whereas those for HLSP and HTB are 120 and 180 minutes, respectively.

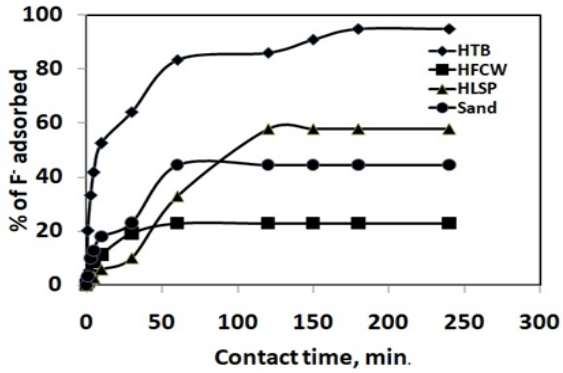

Figure 3. Effect of contact time on F^- adsorption.

4.2.2. Effect of pH.

The effect of pH on F^- adsorption was studied by varying the pH of the solution from 2 to 10. The % F^- adsorptions with respect to pH for all the adsorbents are shown in Figure 4. As shown in the figure, the F^- removal percentage decreases with the increase in pH. It may be due to the change of surface charge on the adsorbent surface [23]. Equations (16-18) are predominant at lower pH. So, the adsorption percentage is more in acidic pH due to the electrostatic force of attraction.

Adsorption of anions on the oxide/hydroxide surface takes place through the formation of surface complexes. Surface complexes are classified into two types depending on the connection between the adsorbate and the active site on the adsorbent surface. These are inner and outer sphere complexes [24]. These surface complexes are formed based on surface protonation/dissociation. For the formation of outer sphere complexes, the reaction is

$$SOH_2^+ (s) + F^- (aq) \leftrightarrow SOH_2^+\text{-}F^- \quad ((19)$$

And for the formation of inner-sphere complexes, the reaction is

$$SOH_2^+ (s) + F^- (aq) \leftrightarrow SF + H_2O \quad (20)$$

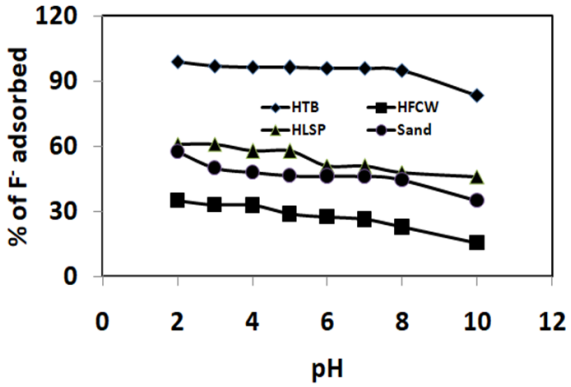

Figure 4. Effect of pH on F^- adsorption.

4.2.3. Effect of adsorbent dose.

The effect of adsorbent dose on F^- adsorption was studied by varying the doses from 5 to 40 g/L. As observed by other researchers here also, % F^- removals increase with adsorbent dosages, whereas uptakes in terms of mg/g decrease. This is due to the availability of more surface area on the adsorbent surfaces at higher adsorbent doses. Maximum F^- removals (%) follow the order HTB (97.66) > HLSP (58.1) > Sand (51.23) > HFCW (42.13). Maximum F^- uptakes (mg/g) also follow the same trend, i.e., HTB (2.88) > HLSP (1.75) > Sand (1.37) >

HFCW (0.84). The variation of F^- adsorption (%) and uptake (mg/g) with respect to adsorbent concentrations are shown in Figure 5.

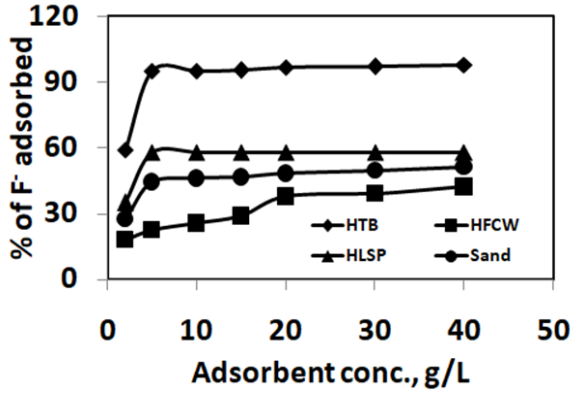

(a)

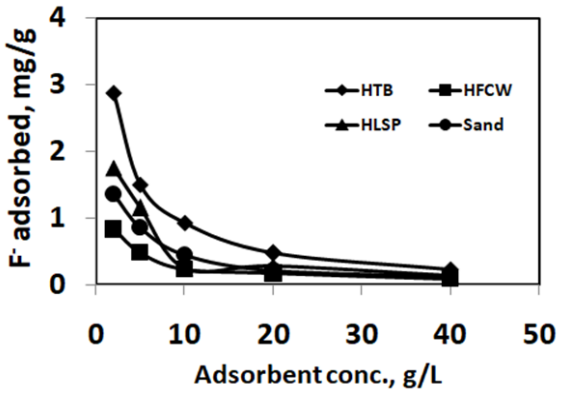

(b)

Figure 5. Effect of adsorbent dose on (**a**) % F^- adsorption;(**b**) F^- uptake, mg/g.

4.2.4. Effect of initial F^- concentration.

The F^- concentration of the solution was varied from 5 to 25 mg/L. Figure 6 shows the effect of variation of F^- concentration on adsorption. The % of F^- adsorption decreases whereas F^- uptakes, mg/g, increase with the increase of F^- concentration for all the adsorbents. At higher F^- concentrations, adsorbent:adsorbate ratio is less. So, the adsorption % is also less. But with the increase of F^- concentration, the probability of contact between adsorbate and a particular amount of adsorbent increases, increasing the F^- uptake capacities. With increased F^- concentration, the repulsive forces arise due to negative charges of F^- also decrease the sorption quantity [25]. Here also, the selectivity order of adsorbents towards F^- is HTB > HLSP > Sand > HFCW.

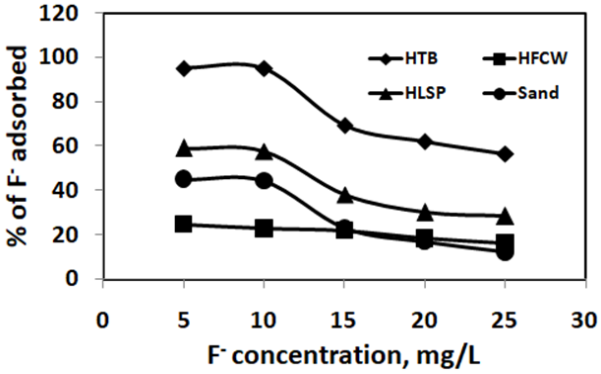

(a)

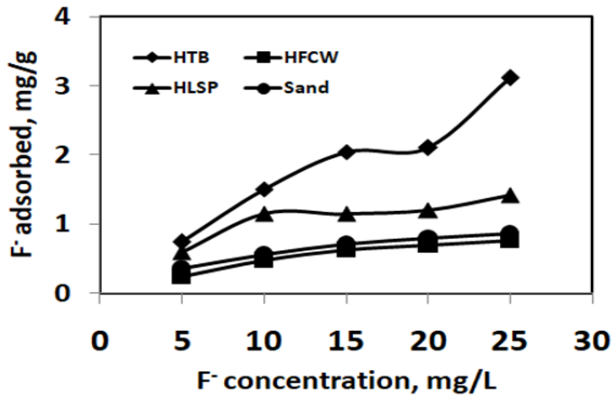

(b)

Figure 6. Effect of adsorbate dose on (**a**) % F^- adsorption (**b**) F^- uptake, mg/g.

4.2.5. Adsorption isotherms.

The Freundlich and Langmuir isotherm constants, along with the standard deviation (S) and separation parameter (R_L) values for F^- adsorption on all the adsorbents, are shown in Table 3. The R^2 values for the Langmuir isotherms are more than that of Freundlich, whereas the standard deviation values of Langmuir isotherms are less than that of Freundlich. So, Langmuir isotherm is obeyed well by all the adsorbents, and Langmuir uptake capacities are considered for comparing the studied adsorbents towards F^- adsorption. Langmuir maximum monolayer uptake capacities (mg/g) of the adsorbents decrease in the order HTB (3.1) > HLSP (1.56) > HFCW (1.55) > Sand (0.63). HTB has the highest uptake capacity, i.e., 3.1 mg/g, compared to other adsorbents. So, HTB is considered the best adsorbent for F^- uptake in the present study. The separation parameter (R_L) values mentioned in Table 3 lie within the range 0 to 1 in all cases except sand, indicating that F^- adsorption on all the adsorbents except the sand is favorable. For sand, it is unfavorable. The Langmuir monolayer adsorption capacities of the studied adsorbents are comparable to that of other low-cost adsorbents and are mentioned in Table 4.

Table 3. Freundlich and Langmuir isotherm constants, along with the correlation coefficients (R^2), standard deviation (S), and separation parameter (R_L) values.

Adsorbents	Freundlich constants				Langmuir constants				
	K, mg/g	n	R^2	S	q_m, mg/g	b	R^2	S	R_L
HTB	1.64	4.4	0.79	0.23	3.1	1.05	0.95	0.01	0.037 to 0.16 (Favorable)
HLSP	0.55	3.02	0.77		1.56	0.35	0.97		0.1 to 0.36 (Favorable)
HFCW	0.10	1.43	0.95		1.55	0.054	0.97		0.42 to 0.79 (Favorable)
Sand	0.53	10.5	0.41		0.63	-2.14	0.98		-0.1 to -0.02 (Unfavorable)

Table 4. Comparison of Langmuir monolayer F^- uptake capacities of the studied adsorbents with that of other reported results.

Low-cost adsorbents	q_m, mg/g	References
HTB	3.1	Present study
HLSP	1.56	Present study
HFCW	1.55	Present study
Sand	0.63	Present study
Natural clay	3.74	[26]

Low-cost adsorbents	q_m, mg/g	References
Microwave-assisted carbonized *Azadirachta indica* bark (MACAIB)	0.92	[27]
Coconut root	2.04	[28]
Low-cost ceramic nodules prepared from some locally available raw materials in Assam, India	6.32	[29]
Activated carbon derived from iron-infused *Pisum sativum* peel	4.71	[19]

4.2.6. Effect of temperature and thermodynamics of adsorption.

F^- adsorption percentages decrease with a rise in temperature (from 30°C to 60°C), as shown in Figure 7. It indicates the reaction to be exothermic. The exothermic nature indicates that the adsorption reactions are physical [30]. At higher temperatures, the solubility of F^- ion increases, and deterioration of adsorbent surfaces may also occur, for which adsorption efficiency decreases [31]. Activation energies were calculated using the Arrhenius equation, whereas other thermodynamic parameters (enthalpy, entropy, and free energy changes) were calculated using the van't Hoff formula. The parameters are shown in Table 5. Out of all the adsorbents, the activation energy for HTB is only negative and lowest. Similarly, the free energy changes on the HTB surface at various temperatures are only negative, which leads to conclude that F^- adsorption on HTB is only spontaneous. The negative values of enthalpy change in all the cases suggested that F^- adsorptions are exothermic, whereas the negative values of entropy changes suggested the achievement of more stability of the adsorption products after adsorption [32].

Table 5. Parameters derived from temperature experiments.

Thermodynamic Parameters		HTB	HLSP	HFCW	Sand
Activation Energy, kJ/mol		-22.8	39.9	27.9	55.05
ΔH, kJ/mol		-48.0	-33.8	-26.0	-41.9
ΔS, kJ/K.mol		-0.15	-0. 12	-0.11	-0.15
ΔG, kJ/mol	303K	-3.2	3.2	7.1	4.7
	313K	-1.7	4.4	8.2	6.2
	323K	-0.2	5.7	9.3	7.7
	333K	1.3	6.9	10.4	9.3

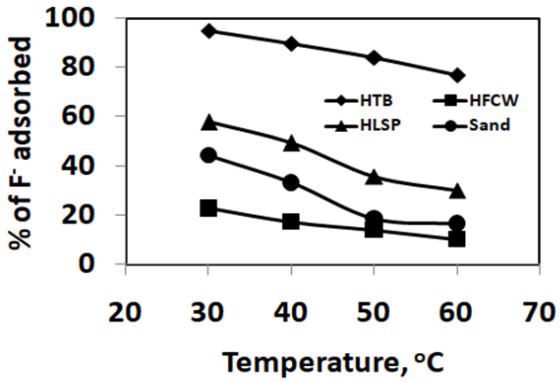

Figure 7. Effect of temperature on F^- adsorption.

4.3.Adsorption kinetics.

The data was interpreted using different kinetic models such as Ho & McKay, Lagergren's, Morris-Weber, Temkin, and Dubinin Radushkevich's (D.R.) isotherms. All the

kinetic parameters are shown in Table 6. The R^2 values of Ho & McKay equations are higher in comparison to Lagergren's equation.

Table 6. Different kinetic equations parameters.

Sl. No.	Adsorbate F^-, mg/L	Adsorbent, g/L	Lagergren's eqn, R^2	Ho & Mc-Kay eqn.		Morris-Weber eqn.		Dubinin-Radushkevich(D.R.) isotherm				Temkin isotherm	
				k_2[a]	R^2	R_{id}[b]	R^2	X'_m[c]	K'[d]	R^2	$E^e=(2K')^{-1/2}$	B[f]	R^2
	HTB												
1	5	5	0.94	0.134	0.99	0.036	0.93	2.52	5×10^{-8}	0.91	3.16	0.40	0.83
2	10	5	0.93	0.058	0.99	0.079	0.93						
3	15	5	0.91	0.021	0.95	0.105	0.91						
4	20	5	0.43	0.013	0.92	0.139	0.87						
5	25	5	0.90	0.007	0.90	0.170	0.78						
	HLSP												
1	5	5	0.92	0.026	0.94	0.067	0.97	1.32	8×10^{-7}	0.94	0.79	0.31	0.8
2	10	5	0.90	0.005	0.92	0.140	0.95						
3	15	5	0.90	0.002	0.94	0.133	0.99						
4	20	5	0.89	0.0009	0.90	0.145	0.97						
5	25	5	0.88	0.0006	0.92	0.174	0.90						
	HFCW												
1	5	5	0.97	0.63	0.99	0.026	0.99	0.75	3×10^{-6}	0.94	0.41	0.33	0.99
2	10	5	0.98	0.17	0.99	0.053	0.97						
3	15	5	0.88	0.25	0.99	0.067	0.98						
4	20	5	0.89	0.08	0.99	0.095	0.95						
5	25	5	0.98	0.034	0.99	0.122	0.99						
	Sand												
1	5	5	0.87	0.21	0.99	0.049	0.97	0.73	6×10^{-7}	0.44	0.92	0.17	0.81
2	10	5	0.82	0.069	0.99	0.107	0.91						
3	15	5	0.84	0.092	0.99	0.07	0.97						
4	20	5	0.80	0.015	0.89	0.091	0.94						
5	25	5	0.80	0.014	0.89	0.102	0.99						

(Units: a - g/mg/min; b- $mg/g/min^{0.5}$; c - mg/g; d - mol^2/J^2; e - kJ /mol; f - J/mol)

So, F^- adsorptions on all the said adsorbents better follow pseudo-second-order kinetics, and the pseudo-second-order rate constant (k2) is considered for different calculations. The rate constants were found to be in the range of 0.6 x 10^{-3} to 0.63 g/mg/min. The data were fitted to the Morris-Weber equation to know the rate-controlling step of adsorption. It has been concluded that the present adsorption processes are controlled by film and intra-particle diffusion [33]. The intraparticle diffusion rate constants (R_{id}) for all the adsorbents have been shown in Table 6. R^2 values of D.R. and Temkin isotherms show a good fit for these isotherms. The adsorption energies calculated from D.R. isotherms fall from 0.41 to 3.16 kJ/mole. It indicates that F^- adsorptions are physisorption type. The heat of sorption values (B) derived from Temkin isotherm falls in the range of 0.17 to 0.40 J/mol, which concludes that the nature of adsorption is physical [34].

The standard deviations (S) were calculated for the uptake capacities of three different isotherms: Langmuir, Freundlich, and D.R. isotherms. S values less than 1 in all the cases, as shown in Table 7, indicate that the observed adsorption data are reliable.

Table 7. Determination of standard deviation (S) for the uptake capacities calculated from different adsorption isotherms.

Isotherm uptake capacities, mg/g	HTB	HLSP	HFCW	Sand
Langmuir	3.1	1.56	1.55	0.63

Isotherm uptake capacities, mg/g	HTB	HLSP	HFCW	Sand
Freundlich	1.64	0.55	0.10	0.53
Dubinin-Radushkevich (D.R.)	2.52	1.32	0.75	0.73
S	0.74	0.53	0.73	0.1

4.4. Best adsorbent selection followed by its regeneration and reuse.

As observed from the present study, F^- uptake on HTB is much higher compared to other adsorbents. It is also very important to note that HTB obeys all the adsorption kinetics/isotherms with good accuracy compared to other adsorbents. And also, HTB is best in terms of its easy availability, low cost, and strength. So, further studies were carried out with HTB. An efficient adsorbent should have good desorption ability to regenerate and be reused several times before its disposal. Therefore, the choice of a good desorbing agent is very much essential. That desorbing agent should also be cheap, highly selective, efficient, and should not deteriorate the adsorbent surface [35]. For the desorption of anionic contaminants like As(V), Cr(VI), F^-, etc., several desorbing agents have been used by different researchers. The desorbing agents are $NaNO_3$, Na_2CO_3, NaOH, etc. [36,37]. In the present investigation, loaded HTB (2.84 mg/g) was used for the desorption experiments. It was observed that desorption with distilled water was very negligible. Desorption experiments were carried out using various eluants (0.1M) such as HCl, H_2SO_4, HNO_3, NaOH, $NaHCO_3$, and Na_2CO_3. It was observed that elution with NaOH (38.7%) was quite successful and best compared to other reagents. This is in agreement with the other reported results [38].

The F^- desorption with NaOH may happen due to the displacement of F^- ions from the adsorbent surface by OH^- of NaOH. After desorption, the adsorbent was washed properly, air-dried at room temperature, and stored for further regeneration and reuse studies. The experimental conditions of the subsequent cycles are the same as that of the 1^{st} cycle. The reusability of HTB was investigated up to 3 more adsorption-desorption cycles. From the result, it is obvious that HTB could be recycled up to 3 times. The % reduction of adsorption capacities in the 2^{nd} and 3^{rd} cycles were 14 and 36%, respectively with respect to the 1^{st} cycle, whereas the % weight losses in the 3 cycles were 10, 19, and 42%, respectively. So, HTB has the potential to be used as an effective adsorbent for wastewater treatment in multi-stages of operation.

4. Conclusions and Future Prospects

The F^- from the synthetic aqueous solution can be removed by all four adsorbents studied here, such as bauxite, LSP, FCW, and sand. Simple heat/acid treatment modifications improved their efficiency, except for sand. Heat treatment at 400^oC worked well for bauxite, whereas HCl treatment was best for LSP and FCW. Low pH favors F^- adsorption, and the optimum contact times for heat-treated bauxite (HTB), hydrochloric acid-treated *Lagenaria siceraria* peel (HLSP), hydrochloric acid-treated water filter carbon waste (HFCW), and sand were found to be 180, 120, 60 and 60 minutes respectively. All the adsorption reactions were exothermic, and the negative entropy changes suggested achieving more stability after adsorption. F^- adsorption on HTB only was found to be spontaneous. Langmuir adsorption capacities were found to be 3.1, 1.56, 1.55, and 0.63 mg/g for HTB, HLSP, HFCW, and sand, respectively. These uptake values are comparable with that of other low-cost adsorbents. Heat-

treated bauxite (HTB) was found to be the best adsorbent out of all. The F^- loaded HTB can be regenerated using 0.1M NaOH and can be reused for up to 3 cycles.

The present method of removal of F^- using low-cost materials is a method of options and combinations, and the option is vast. Based on the present investigations, cheaper and cheaper novel materials can be tested and compared with already reported materials. Even if great research is going on in this field, the treatment of real contaminated water using various adsorbents is not yet well reported. Most of the research is carried out using synthetic solutions. It cannot evaluate the adsorption efficiency of a particular adsorbent truly. Using low-cost adsorbents for the treatment of real contaminated water would be an effective and fruitful method if continuous research was carried out in the same field. The present small-scale batch adsorption studies can be further extended to continuous column studies for treating real F^- polluted industrial wastewater.

Funding

This research received no external funding.

Acknowledgments

One of the authors (Ghosh) thanks Siksha 'O' Anusandhan (Deemed to be University) for the research fellowship. The authors are thankful to Siksha 'O' Anusandhan (Deemed to be University), Bhubaneswar, for giving constant support and permission to publish this paper.

Conflicts of Interest

The authors declare no conflict of interest.

References

1 Karunanithi, M.; Agarwal, R.; Qanungo, K. A review of fluoride removal from groundwater, *Period. Polytech. Chem. Eng*. **2019**, *63*, 425–437, https://doi.org/10.3311/PPch.12076.
2. Kashyap, S.J.; Sankannavar, R.; Madhu, G.M. Fluoride sources, toxicity and fluorosis management techniques – A brief review, *J. Hazard. Mater. Lett.***2021**, *2*, 100033, https://doi.org/10.1016/j.hazl.2021.100033.
3. Moses, E.; Grace, B. Fluoride contamination and its optimum upper limit in groundwater from Sukulu hills, Tororo District, Uganda, *Sci. Afr.***2020**, *7*, e00241, https://doi.org/10.1016/j.sciaf.2019.e00241.
4. Dey, S.; Giri, B. Fluoride fact on human health and health problems: A Review, *Med. Clin. Rev.***2015**, *2*, 2,https://doi.org/10.21767/2471-299X.1000011.
5. Tolkou, A.K.; Manousi, N.; Zachariadis, G.A.; Katsoyiannis, I.A.; Deliyanni, E.A. Recently developed adsorbing materials for fluoride removal from water and fluoride analytical determination techniques: A review, *Sustainability***2021**, *13*, 7061, https://doi.org/10.3390/su13137061.
6. Tesfaye, A., Achalu, C., Kefyalew, G. Removal of fluoride from drinking water by sorption using diatomite modified with aluminum hydroxide, *J. Anal. Methods. Chem.***2019**, *2019*, 4831926, https://doi.org/10.1155/2019/4831926.
7. Hania A.; Hazim Q.; Muftah H.E. Comparative study between adsorption and membrane technologies for the removal of mercury, *Sep. Purif. Technol*. **2021**, *257*, 117833,https://doi.org/10.1016/j.seppur.2020.117833.
8. Mishra, S.P. Insights into the recent use of modified adsorbents in removing heavy metal ions from aqueous solution, *Biointerface Res. Appl. Chem.* **2022**, *12*, 1884-1898,https://doi.org/10.33263/BRIAC122.18841898.
9. Kalsido, A.W.; Kumar, A.; Tekola, B.; Mogessie, B.; Alemayehu, E. Evaluation of bentonite clay in modified and unmodified forms to remove fluoride from water, *Water Sci. Technol.***2021**, *84*, 2661–2674, https://doi.org/10.2166/wst.2021.220.
10. Sahu, N.; Bhan, C.; Singh, J. Removal of fluoride from an aqueous solution by batch and column process using activated carbon derived from iron infused*Pisum sativum*peel: characterization, isotherm, kinetics study, *Env. Eng. Res.***2021**, *26*, 200241,https://doi.org/10.4491/eer.2020.241.
11. So˘co, E.; Papciak, D.; Michel, M.M.; Paj ˛ak, D.; Domon, A.; Kupiec, B. Characterization of the physical, chemical, and adsorption properties of coal-fly-ash– hydroxyapatite composites, *Minerals***2021**, *11*, 774, https://doi.org/10.3390/min11070774.

12. Hashemkhani, M.; Rezvani Ghalhari, M.; Bashardoust, P.*et al.*Fluoride removal from aqueous solution via environmentally friendly adsorbent derived from seashell.*Sci. Rep.***2022**, *12*,9655, https://doi.org/10.1038/s41598-022-13756-3.
13. Kaushal, A., Singh, S.K. Critical analysis of adsorption data statistically, *Appl. Water Sci.***2017**, *7*, 3191–3196, https://doi.org/10.1007/s13201-016-0466-4.
14. Dada, A.O.; Adekola, F.A.; Odebunmi, E.O.*et al.*Two–three parameters isotherm modeling, kinetics with statistical validity, desorption and thermodynamic studies of adsorption of Cu(II) ions onto zerovalent iron nanoparticles,*Sci. Rep.***2021**, *11***,**16454, https://doi.org/10.1038/s41598-021-95090-8.
15. Ghosh, M.R.; Mishra S.P. Adsorption of Cr(VI) by using HCl modified *Lagenaria siceraria* peel (HLSP), *J. Mater. Environ. Sci.***2016**, *7*, 3050-3060, https://doi.org/10.1016/j.jece.2019.103641.
16. Urai, J.L.; Feenstra, A. Weakening associated with the diaspore–corundum dehydration reaction in metabauxites: an example from Naxos (Greece), *J. Struct. Geol.* **2001**, *23*, 941–950, http://dx.doi.org/10.1016/S0191-8141(00)00165-6.
17. Achary, P.G.R.; Ghosh, M.R.; Mishra, S.P. Insights into the modeling and application of some low cost adsorbents towards Cr(VI) adsorption, *Mater. Today Proc.* **2020**, *30*, 267–273, https://doi.org/10.1016/j.matpr.2020.01.433.
18. Hadjiivanov, K. Identification and characterization of surface hydroxyl groups by infrared spectroscopy, *Adv. Catal.* **2014**, *57*, 99-318, http://dx.doi.org/10.1016/B978-0-12-800127-1.00002-3.
19. Iizuka, A.; Ho, H-J.; Yamasaki, A. Removal of fluoride ions from aqueous solution by metaettringite, *PLoS ONE*, **2022**, *17*, e0265451, https://doi.org/10.1371/journal.pone.0265451.
20. Roy, T.;Wisser, D;Rivallan, M.;Valero, M.C.; Corre, T.; Delpoux, O.; Pirngruber, G.D.; Lefèvre, G. Phosphate adsorption on γ-alumina: A surface complex model based on surface characterization and zeta potential measurements, *J. Phys. Chem. C* **2021**, *125*, 10909–10918,https://doi.org/10.1021/acs.jpcc.0c11553.
21. Gale, M.; Nguyen, T.; Moreno, M.; Gilliard-AbdulAziz, K.L.Physiochemical properties of biochar and activated carbon from biomass residue: influence of process conditions to adsorbent properties, *ACS Omega***2021**, *6*, 10224–10233, https://doi.org/10.1021/acsomega.1c00530.
22. Mishra, S.P.; Patra, A.R.; Das, S. Methylene blue and malachite green removal from aqueous solution using waste activated carbon, *Biointerface Res. Appl. Chem.* **2021**, *11*, 7410-7421, .http://dx.doi.org/10.33263/BRIAC111.74107421.
23. Peterson, S.C.; Kim, S.; Adkins, J. Surface charge effects on adsorption of solutes by poplar and elm biochars, *J. C Res.* **2021**, *7*, 11, https://doi.org/10.3390/c7010011.
24. Lambert R.L.; Manuel T.A. O,O' Diphenyl dithio phosphate tetracarbonyl manganese(I) and related compounds, *Inorg. Chem.* **1966**, *5*, 1287–1289, https://doi.org/10.1021/ic50041a051.
25. Belhaj, A.F.; Elraies, K.A.; Mahmood, S.M. The effect of surfactant concentration, salinity, temperature, and pH on surfactant adsorption for chemical enhanced oil recovery: a review, *J. Petrol Explor. Prod. Technol.* **2020**, *10*, 125–137, https://doi.org/10.1007/s13202-019-0685-y.
26. Nabbou, N.; Belhachemi, M.; Boumelik, M.; Merzougui, T.; Lahcene, D.; Harek, Y.; Zorpas, A.A.; Jeguirim, M. Removal of fluoride from groundwater using natural clay (kaolinite): Optimization of adsorption conditions, *Comptes Rendus Chimie*, **2019**, *22*, 105-112, https://doi.org/10.1016/j.crci.2018.09.010.
27. Telkapalliwar, N.G.; Shivankar, V.M. Data of characterization and adsorption of fluoride from aqueous solution by using modified *Azadirachta indica* bark, *Data Brief*, **2019**, *26*, 104509, https://doi.org/10.1016/j.dib.2019.104509.
28. George, A.M.; Tembhurkar, A.R. Analysis of equilibrium, kinetic, and thermodynamic parameters for biosorption of fluoride from water onto coconut (*Cocos nucifera* Linn.) root developed adsorbent, *Chin. J. Chem. Eng.* **2019**, *27*, 92–99, https://doi.org/10.1016/j.cjche.2018.03.004.
29. Saikia, J.; Sarmah, S.; Hussain Ahmed, T.; Kalita, P.J.; Goswamee, R.L. Removal of toxic fluoride ion from water using low cost ceramic nodules prepared from some locally available raw materials of Assam, India, *J. Env. Chem. Eng.* **2017**, *5*, 2488-2497, https://doi.org/10.1016/J.JECE.2017.04.046.
30. Al-Ghouti, M.A.; Al-Absi, R.S. Mechanistic understanding of the adsorption and thermodynamic aspects of cationic methylene blue dye onto cellulosic olive stones biomass from wastewater, *Sci. Rep*. **2020**, *10*, 15928, https://doi.org/10.1038/s41598-020-72996-3.
31. Rapo, E.; Tonk, S. Factors affecting synthetic dye adsorption; desorption studies: A review of results from the last five years (2017–2021), *Molecules*, **2021**, *26*, 5419, https://doi.org/10.3390/molecules26175419.
32. Palmay, P.; Puente, C.; Barzallo, D.; Bruno, J.C. Determination of the thermodynamic parameters of the pyrolysis process of post-consumption thermoplastics by non-isothermal thermogravimetric analysis, Polymers **2021**, *13*, 4379, https://doi.org/10.3390/polym13244379.
33. Hwang, K.J.; Shim, W.G.; Kim, Y.; Kim, G.; Choi, C.; Kang, S.O.; Cho, D.W. Dye adsorption mechanisms in TiO_2 films, and their effects on the photodynamic and photovoltaic properties in dye-sensitized solar cells, *Phys. Chem. Chem. Phys.* **2015**, *17*, 21974-21981, https://doi.org/10.1039/C5CP03416G.
34. Nnaji, C.C.; Agim A.E.; Mama, C.N.; Emenike, P.C.; Ogarekpe, N.M.Equilibrium and thermodynamic investigation of biosorption of nickel from water by activated carbon made from palm kernel chaf, *Sci. Rep*. **2021**, *11*, 7808, https://doi.org/10.1038/s41598-021-86932-6.

35. Hamad, H.N.; Idrus, S. Recent developments in the application of bio-waste-derived adsorbents for the removal of methylene blue from wastewater: A review, *Polymers* **2022**, *14*, 783, https://doi.org/10.3390/polym14040783.
36. Sawangjang, B.; Induvesa, P.; Wongrueng, A.; Pumas, C.; Wattanachira, S.; Rakruam, P.; Punyapalakul, P.; Takizawa, S.; Khan, E. Evaluation of fluoride adsorption mechanism and capacity of different types of bone char. Int. J. Environ. Res. Public Health., **2021**, *18*, 6878, https://doi.org/10.3390/ijerph18136878.
37. Amin, F.; Talpur, F.N.; Balouch, A.; Surhio, M.A.; Bhutto, M.A. Biosorption of fluoride from aqueous solution by white—rot fungus *Pleurotus eryngii* ATCC 90888, *Environ. Nanotechnol. Monit. Manag.* **2015**, *3*, 30–37, https://doi.org/10.1016/j.enmm.2014.11.003.
38. Jiang, K.; Zeng, X. Desorption and recovery of fluoride adsorbed by the aluminum-loaded chelating resin, Desalin. Water Treat. **2021**, *224*, 178–186, https://doi.org/10.5004/dwt.2021.27128.